Post-Flood Paleoclimate: Reexamining the Sediment and Ice Core Records in Light of the Global Flood

Kadyn Kunisaki*

Key Words: Cenozoic Era, Climate Change, Global Flood, Ice Age, Paleoclimatology

* Kadyn Kunisaki, Mililani, HI, itskayla808@gmail.com

Accepted for publication November 11, 2024

Abstract

The term *climate change* is widely used but often understates the severity projected in secular climate literature. Within mainstream science, *climate change* frequently functions as shorthand for *catastrophic climate change*, with careful phrasing employed to minimize questioning of the prevailing consensus. The observational record does indicate a clear warming trend since the mid-twentieth century; however, creationists do not dispute these data. Instead, the point of contention lies in the secular interpretation of paleoclimate records, particularly those extending far beyond the period of human observation. This paper reexamines Cenozoic Era sediment and ice core records, which secular scientists cite as evidence for catastrophic climate change. It will be shown that the Biblical record—specifically the Global Flood and post-Flood Ice Age—offers a superior explanatory framework for paleoclimate data, challenging the historical basis for climate alarmism.

Simple Summary

This article suggests that understanding Earth's past climate, called paleoclimatology, is more accurate when viewed through the Biblical story of the Global Flood and the Ice Age that followed, instead of the common scientific view. Mainstream science assumes Earth is millions of years old and uses information from ancient sediment and ice to warn about "catastrophic climate change." However, this paper argues that these interpretations are mistaken. By taking the *same* climate data and re-dating it to fit a Biblical timeline (for example, placing the Global Flood around 4,375 years ago), the author believes that very warm periods in Earth's past were actually part of the warm global climate during and right after the Flood. He explains that the quick cooling seen in the data after the Flood was due to widespread volcanic activity and increased evaporation, which then led to a single Ice Age. While secular scientists suggest many different reasons for climate shifts over long periods, this study proposes that the Global Flood is the main, powerful event that explains the entire paleoclimate record. The author concludes that worries about catastrophic human-caused climate change are based on an incorrect understanding of Earth's climate history, emphasizing God's promise that such a global catastrophe will not happen again.

Disclaimer: *According to Mike Oard, creation scientists have not thoroughly examined the deep-sea sediments used in this study (Oard, 2024, personal communication). The intent is simply to show that the secular climate reconstruction, even with its circular reasoning and favorable dating practices, better fits the Biblical framework.*

Introduction

Paleoclimatology provides insight into Earth's climate history and is widely used by secular scientists to calibrate climate models, assess climate sensitivity, and develop analogs for future climate states. On the surface, this appears neutral, as understanding past climates can help predict future trends. However, if secular assumptions—particularly uniformitarianism and its millions-of-years' timeline—are inaccurate, then paleoclimate reconstructions reflect a fundamentally flawed interpretation of the past. This study addresses that issue by reframing Cenozoic paleoclimatology within a Biblical framework. The paper begins by describing the methodology and datasets employed, followed by a summary of the secular interpretation of the paleoclimate record. It concludes with a reinterpretation of the record according to the Biblical timeline. While secular research struggles to converge on a consensus regarding the primary drivers of past climate changes, the Biblical framework provides a coherent explanation, connecting the paleorecord directly to the catastrophic Global Flood.

Methodology

The paleoclimate reconstructions in this study are derived from stacked deep-sea benthic foraminiferal oxygen-isotope curves (Lisiecki and Raymo, 2005; Zachos et al., 2008) and high-resolution deuterium (stable hydrogen isotope) profiles from the European Project for Ice Coring in Antarctica (EPICA) Dome C ice core record (Jouzel et al., 2007). The first two curves (Lisiecki and Raymo, 2005; Zachos et al., 2008), covering 65 Ma to 100 ka, were translated into temperature profiles using the Hansen et al. (2013) prescription, which converts deep sea oxygen isotope ratios to sea surface temperatures. This prescription generates profiles mirroring figures in Hansen et al. (2013) and Haywood et al. (2019). For the EPICA Dome C ice core record, the temperature profile, covering 100 ka to 70 years before present, is based on the conversion of stable hydrogen isotope measurements. Reported values in Jouzel et al. (2007) were divided by a standard amplification factor to convert polar to global temperatures (Hansen et al., 2013).

Original data from Zachos et al. (2008), Lisiecki and Raymo (2005), and Jouzel et al. (2007) were dated using the secular timeline; therefore, the paleoclimate reconstructions in Figure 1 extend back to ~65 Ma. To reframe the temperatures into the Biblical framework, primary reference horizons (ie.Flood/post-Flood Boundary, Glacial Maximum, Ice Age End) in the reconstruction were dated using the Masoretic Text (Wright, 2012), as well as the timeline for the post-Flood Ice Age (Oard, 2019). The data points following the Flood/post-Flood Boundary were linearly interpolated between reference horizons. From this methodology, it is important to mention that any climate data before the Flood/post-Flood Boundary reflects a high level of uncertainty because of turbulent sedimentation occurring during the Flood year. After the Flood/post-Flood Boundary though, sedimentation rates subside to near-uniformity, which allows for a more accurate conversion of oxygen isotope ratios to surface temperature.

The use of linear interpolation assumes that sedimentation rates reached uniformity immediately following the Flood/post-Flood Boundary. While a simplifying assumption, it is sufficient for illustrating post-Flood temperature trends to first approximation. Maximum and minimum temperatures at the post-Flood Boundary and Glacial Maximum provide upper and lower bounds for estimating the overall post-Flood cooling rate. Future studies may refine this approach by considering non-linear sedimentation decay rates following the Flood/post-Flood Boundary, potentially applying Vardiman (1996)'s exponential model.

Data Availability Statement: Datasets for this study were retrieved from the website Real Climate, which provides data for Zachos et al. (2008), Lisiecki and Raymo (2005), and Jouzel et al. (2007), as well as other temperature reconstructions extending back to the hypothetical Cambrian Period (Schmidt, 2014).

Oxygen Isotope Ratios

Before discussing secular versus Biblical interpretations of the paleoclimate record, it is important to understand isotope ratios and their correlation to temperature. Oxygen, for example, has three stable isotopes: ^{16}O, ^{17}O, and ^{18}O. These occur in the atmosphere in proportions of approximately 99.757%, 0.038% and 0.205%, respectively (Rosman and Taylor, 1998). Using the global average proportion of the heavier ^{18}O isotope to the lighter ^{16}O isotope (0.205/99.757), scientists can determine oxygen isotope ratio deviations ($\delta^{18}O$) for different periods in the record. Theoretically, this deviation provides information about the environment when and where the record formed. In uniformitarian thought, the precipitation rate is proportional to the temperature throughout the record; therefore, the isotope ratio accurately details past precipitation rates and temperatures (Oard, 2005).

Issues do preclude a straightforward conversion of $\delta^{18}O$ into temperature values though. Many variables, such as the oxygen isotope ratio of evaporating seawater, the distance of travel for moisture from its source region, and precipitation intensity, complicate the use of isotope ratios as a temperature proxy, specifically during the Pleistocene Ice Age (Vardiman, 1997; Oard, 2020). Additionally, there is debate about whether $\delta^{18}O$ values are better interpreted as a function of environmental temperature or ice sheet extent (Oard, 1984; Hebert, 2014). Despite these factors, this study presumes that isotope ratios are an effective proxy for relaying relative warming and cooling trends in paleoclimates following the Flood/post-Flood Boundary.

A second issue with paleoclimate records, specifically those derived from sediment and ice cores, is circular reasoning in dating reference horizons (Hebert, 2014). While concerns are warranted regarding chemical "wiggles"

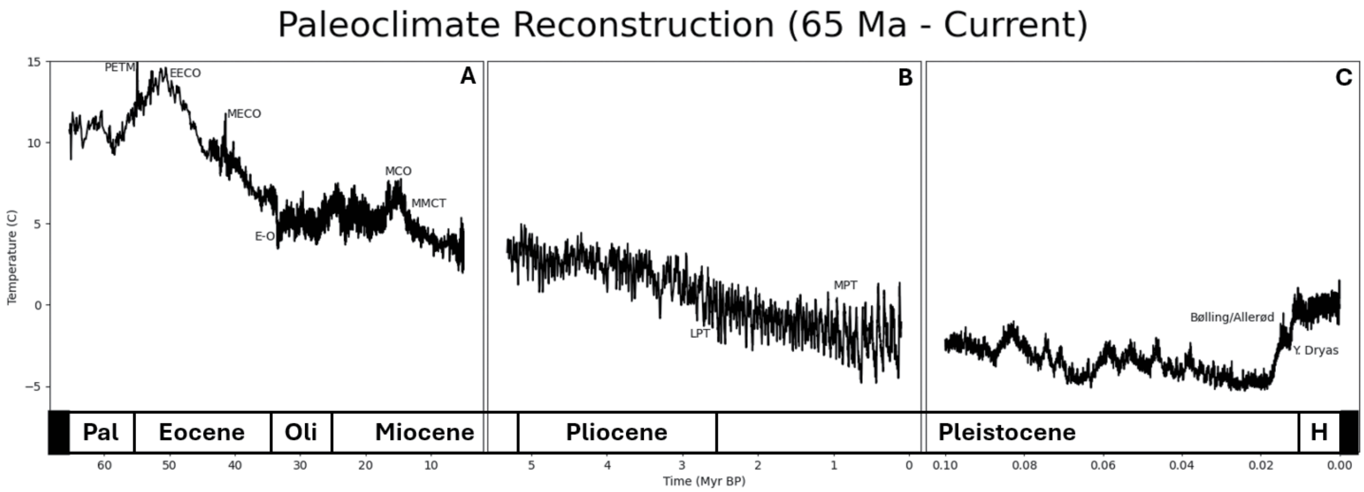

Figure 1. Secular paleoclimate reconstruction from the Paleocene to Holocene. Box A displays data from Zachos et al. (2008), Box B displays data from Lisiecki and Raymo (2005), and Box C displays data from Jouzel et al. (2007). Each major climatic event (labelled in figure) is covered in detail within the paper. The 0°C line on the temperature axis is based on the Pre-Industrial Average.

in Cenozoic sediments, as well as supposed glacial-interglacial cycles of the Pleistocene Ice Age, the relative ages of reference horizons provide a general idea of when warm and cool climates occurred in Earth history. Using these relative dates from secular studies, the paleoclimate record can be reinterpreted into a Biblical framework. Conceptually, this aligns with Vardiman (1996) where the sediment record following the Cretaceous/Tertiary Boundary was reinterpreted using a young Earth framework, albeit Vardiman (1996) used an exponential decay rate for sedimentation following his Flood/post-Flood Boundary.

Primary Assumptions: Following the Flood/post-Flood Boundary, isotope ratios in sediment and ice core records provide a reasonably accurate assessment of temperature trends and relative dating in paleoclimate reconstructions.

Paleoclimatology–Secular Framework

The following section presents the secular framework for paleoclimate reconstructions. Its purpose is to highlight the extensive research conducted on each identified "major climate change" while emphasizing that, despite the volume of study, there remains no consensus regarding the primary causal mechanisms driving these events.

Eocene Epoch

The Eocene Epoch (approximately 56–33.9 Ma) was the warmest period in the Cenozoic Era (Zachos et al., 2008). This was an interval of significant atmospheric CO_2 concentration (minimum 1,125 p.p.m.v., parts per million by volume), consisting of warm climatological features, such as the Paleocene-Eocene Thermal Maximum (PETM), the Early Eocene Climatic Optimum (EECO), and the Middle Eocene Climatic Optimum (MECO). The Eocene Epoch also marked the initial transition from greenhouse to icehouse climate, otherwise known as the Eocene-Oligocene (E-O) Transition (~33.7 Ma). These four features are highlighted in Figure 1a, a temperature conversion based on Zachos et al. (2008).

Paleocene-Eocene Thermal Maximum

The PETM (~56.3 Myr ago), a transient hyperthermal (or rapid warming event) embedded in the warming trend of the Early Eocene, is thought to have lasted 200 kyr with a global temperature increase of 5–8°C, all of which occurred in less than 10,000 years (Zachos et al., 2008; McInerney and Wing, 2011). One study estimated the average global mean surface temperature increased to 31.6°C during this period (Inglis et al., 2020).

The PETM coincides with significant carbon release, verified by a large negative carbon isotopic excursion (CIE), as well as dissolution of deep-ocean carbonates. Secular scientists have proposed many carbon sources, such as methane hydrates and permafrost, to explain the 10,200 petagrams (10^{15}) of carbon (PgC) released during the PETM; however, many recent studies suggest that volcanism better explains the increase (Gutjahr et al., 2018; Tierney et al., 2019; Haynes and Honisch, 2020). Gutjahr et al. (2018) stated:

> "We find strong evidence for a much larger (>10,000 PgC) and on average isotopically heavier carbon source than considered previously. This leads us to identify volcanism associated with the North Atlantic Igneous Province (NAIP), rather than carbon from a surficial reservoir, as the main driver of the PETM" (Gutjahr et al., 2018).

Jones et al. (2019) proposed another feature of the NAIP—methane produced by sub-horizontal sheets of magma—as the most likely source for the large mass of carbon released during the PETM. In modelling, lateral mantle flow rates were 100–200 mm yr^{-1} above current flow speeds in the NAIP sill province, which allowed for high magma production rates and rapid release of carbon into the atmosphere and shallow oceans (Jones et al., 2019).

Although the consensus view for the cause of warming during the PETM is carbon release from volcanism, a few studies have offered astronomical (or Milankovitch) cycles as another potential mechanism for the onset of the PETM (Li et al., 2022; Piedrahita et al., 2022). This follows from studies suggesting that warming preceded the release of carbon by several thousand years (Slujis et al., 2007; Slujis et al., 2011). If accurate, these relegate NAIP volcanism to a long-term positive feedback mechanism during the Eocene Epoch rather than a causal mechanism (Jones et al., 2019). This does not negate CO_2's role in warming; however, it does highlight an unknown initial cause for the PETM.

Early Eocene Climatic Optimum

Occurring between 53–51 Ma, the EECO resides at the primary peak of the Late Paleocene to Early Eocene warm period. One estimate calculated the average global mean surface temperature during the period was 27°C, approximately 14°C warmer than the pre-industrial average (Inglis et al., 2020). Considered a product of increased CO_2 levels, the EECO's concentration is estimated at 1400ppm, although published values range anywhere from 500–3000ppm (Anagnostou et al., 2016).

Two primary causes have been suggested for EECO warming: transient hyperthermal events, such as the PETM, Eocene Thermal Maximum (ETM)-2, and ETM-3, and enormous volcanic eruptions, such as those associated with the Pana Formation in Southern Tibet (Lauretano et al., 2015; Zhang et al., 2023). Both naturally lead to increases in atmospheric CO_2 concentration, and therefore, can theoretically explain the long-term warming associated with this period.

Middle Eocene Climatic Optimum

The MECO, which began approximately 40.6 Ma with peak warming at 40 Ma, marked a rapid reversal of the long-term cooling that began following the EECO (Bohaty et al., 2009). The MECO was a period of high CO_2 concentrations (as high as 4000 ppmv) and global warming, exhibiting a 4–6°C increase in surface and deep ocean temperatures (Bohaty et al., 2009; Pearson, 2010). Immediately following the short lived MECO, the climate experienced a rapid cooling with subsequent return to pre-MECO temperatures within 200 kyr (Bohaty et al., 2009).

The cause of the MECO is still debated. A study by Bohaty and Zachos (2003) suggested either metamorphic decarbonation in the Himalayan orogeny or ridge volcanism associated with plate reorganization as the mechanism for the transient rise in CO_2 levels. Another study suggested a volcanic arc flare-up in the Neotethys subduction zone causing massive volcanism in Iran and Azerbaijan (van der Boon et al., 2021). This follows from the dating of Eocene rocks in Iranian volcanic provinces around 40 Ma (van der Boon et al., 2021). Van der Boon et al (2021) also estimated a total CO_2 release between 1052 and 12,565 PgC, which is compatible with MECO carbon release. Still other studies suggest Milankovitch cycles as the cause of MECO warming (Westerhold and Rohl, 2013; Giorgioni et al., 2019).

Eocene-Oligocene Transition

According to Coxall and Pearson (2007), The E-O Transition was a major period of climate change at 33.7 Ma that lasted approximately 500 kyr. Characterized by a +1.5 per mil rise in oxygen isotopic values of benthic foraminifera, the E-O Transition marked the initial shift from greenhouse to icehouse climate (Liu et al., 2009; Hren, 2013). It also marked the first semi-permanent continental scale Antarctic ice sheets (Coxall and Pearson, 2007).

The cause of the E-O Transition is widely debated; however, three possible mechanisms are often invoked: declining greenhouse gases, the opening of the Southern Ocean gateway allowing Antarctic ice build-up, and Milankovitch cycles (Coxall and Pearson, 2007; Katz et al., 2008; Hren, 2013). Although there seems to be agreement that all three played a role in the transition, many studies suggest that either the CO_2 concentrations reached levels that ultimately triggered rapid ice expansion on Antarctica or that ice expansion led to CO_2 sequestration (Deconto and Pollard, 2003; Pagani et al., 2005; Hren et al., 2013). Regardless, CO_2 concentrations during the Late Eocene Epoch, which ranged between 1000 and 1500 ppmv, rapidly decreased to current concentrations during the Late Oligocene (Pagani et al., 2005).

Miocene Epoch

The E-O Transition marked the initial shift from greenhouse to icehouse climate; however, the Miocene Epoch (23–5 Ma) that followed exhibited a dynamic climate of early and late glaciation interrupted by a 2 Myr greenhouse interval known as the Miocene Climatic Optimum (MCO) (Steinthorsdottir et al., 2020). The general trend of the Miocene (and Pliocene) Period(s) though was a gradual cooling culminating in the Pleistocene Ice Age. Figure 1b shows the two primary features of the Miocene Epoch: the MCO and the Middle Miocene Climatic Transition (MMCT).

Miocene Climatic Optimum

The MCO, which occurred between 17–14 Ma, was a period of global warming ~3–4°C above present temperatures (Sosdian et al., 2020). A phase of relatively high CO_2 concentration (470–630 ppm), the MCO is considered a strong analog for future climates following the Intergovernmental Panel on Climate Change (IPCC)'s Representative Concentration Pathway (RCP) 4.5 or RCP 6.0 scenarios (Sosdian et al., 2020; Steinthorsdottir et al., 2020).

Many studies suggest the MCO was caused by enhanced volcanism and magmatism associated with the Columbia River Basalt Group (CRBG) (Mckay et al., 2014; Kasbohm and Schoene, 2018; Sosdian et al., 2020). Three lines of evidence support this theory: first, during this period, a total of 4090–5670 PgC was released into the atmosphere, which when included with cryptic degassing of the large igneous province, largely reproduced the atmospheric CO_2 change observed during the MCO (Mckay et al., 2014). Second, data showed that 95% of the CRBG erupted between 16.7 and 15.9 Ma, near the peak of the MCO (Kasbohm and Schoene, 2018). Finally, seafloor magnetic records indicate high crustal production rates between 19 and 14 Ma (Goto et al., 2023).

Middle Miocene Climatic Transition

Following the MCO, the MMCT ushered in a sustained icehouse climate at approximately 14 Ma (Raitzsch et al., 2021). The MMCT was marked by the expansion of the East Antarctic Ice Sheet, as well as a large positive CIE (~1‰) (Raitzsch et al., 2021).

Despite the well-documented isotopic record of the Miocene Epoch, the cause of the MMCT is still highly debated. Some studies have suggested the MMCT followed from the final closure of the Tethys Seaway, a prehistoric ocean that separated Laurasia and Gondwana (Woodruff and Savin, 1989; Wright et al., 1992). However, a recent study concluded that the closure of the Tethys Sea was not the main driver of global cooling and Antarctic Ice Sheet expansion (Hamon et al., 2013). Instead, Hamon et al. (2013) suggest the initiation of the MMCT stemmed from pCO_2 drawdown.

CO_2 decrease during the Miocene Epoch corresponds to the Monterey CIE. The classic interpretation, known as the "Monterey Hypothesis," proposed that long-term cooling invigorated upwelling leading to increased carbon burial rates along the Pacific margins (Vincent and Berger, 1985). However, a more recent study suggested the Monterey CIE CO_2 drawdown arose from increased chemical weathering rates (Raymo, 1994). According to Raymo (1994), "The increased supply of nutrients stimulated productivity in oceanic upwelling zones…leading to enhanced burial and preservation of organic matter in the Monterey Formation and other deposits." This interpretation differs slightly from the "Monterey Hypothesis" in that carbon burial is driven by nutrient delivery to the oceans rather than upwelling (Raymo, 1994).

Pliocene-Pleistocene Epoch

The Pliocene and Pleistocene Epochs, referred to as the Plio-Pleistocene, began approximately 5.3 Ma and lasted until 11.7 ka (Jimenez-Moreno et al., 2019). A period of gradual cooling, the Plio-Pleistocene culminated in the most recent Ice Age, characterized by cyclical glacial–interglacial oscillations. Figure 1b, a temperature conversion based on Lisiecki and Raymo (2005), and Figure 1c, a temperature conversion based on Jouzel et al. (2007), show the temperature reconstruction of the Plio-Pleistocene, highlighting three major events: the Late Pliocene Transition (LPT), the Middle Pleistocene Transition (MPT), and the Pleistocene Glacial Retreat (PGR).

Late Pliocene Transition

The Pliocene Epoch is typically broken into two stages: the Zanclean stage (5.3–3.6 Ma) and the Piacenzian stage (3.6–2.6 Ma) (De Schepper et al., 2014; Jimenez-Moreno et al., 2019). The Zanclean, or Early Pliocene, encompasses the Pliocene Climatic Optimum (PCO), a period of global average temperatures approximately 4°C higher than today and CO_2 concentrations around 410 ppm (Bartoli et al., 2011). The Piacenzian, or Late Pliocene, contains the LPT (Lawrence et al., 2010). During the LPT, CO_2 concentrations decreased by about 100 ppm, which led to significant glaciation in both northern and southern hemispheres (Bartoli et al., 2011; De Schepper et al., 2014).

Two primary mechanisms have been proposed for the LPT: altered heat transport from ocean gateway closures and decreased atmospheric CO_2 (Lawrence et al., 2010). For altered heat transport, Lawrence et al. (2010) stated:

> "The closure of two low latitude ocean gateways, the Panamanian Seaway and the Indonesian Throughflow, have figured prominently in arguments for altered heat transport as the explanation for the end of the Early Pliocene warm period."

Regarding CO_2 concentrations, modest concentration decreases were observed during the LPT; however, associated global cooling allowed for the appearance of sizable ice sheets in the Northern Hemisphere, which

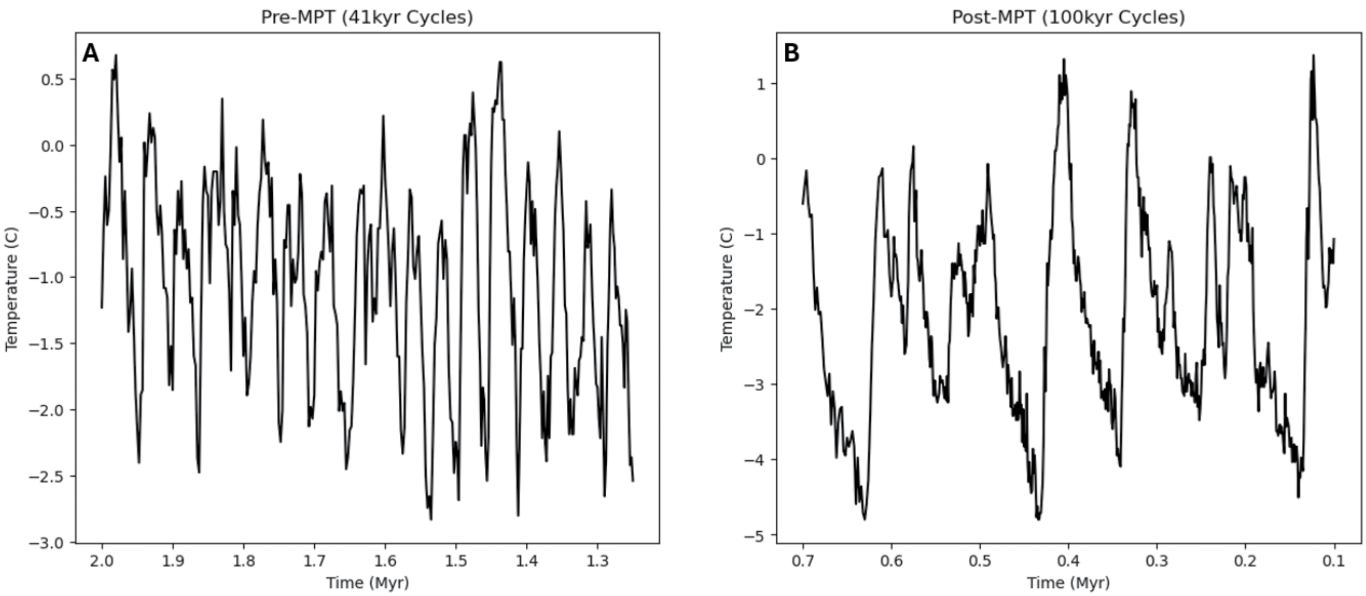

Figure 2. Change in periodicity following the Middle Pleistocene Transition from 41-kyr to 100-kyr cycles. The 0°C line on the temperature axis is based on the Pre-Industrial Average.

intensified the ice-albedo feedback mechanism amplifying regional cooling (Lawrence et al., 2010).

Middle Pleistocene Transition

The MPT, which occurred between 1.25 and 0.7 Ma, marked the major transition in glacial-interglacial cycles from 41-kyr symmetric to 100-kyr asymmetric periods (Willeit et al., 2019). The MPT also brought on "longer, colder, and dustier late Pleistocene ice ages with larger continental ice sheets and lower global sea level" than pre-MPT glacial periods (Chalk et al., 2017). Figures 2a–b show the glacial-interglacial cycles pre- and post-MPT.

The MPT occurred without any major variations in orbital forcing; therefore, the changes to periodicity in glacial-interglacial cycles arose from internal responses of the climate system rather than external forcings (Chalk et al., 2017; Farmer et al., 2019). Internal responses typically fall into one of two categories: ice sheet dynamics or global energy budget adjustments (Chalk et al., 2017). Regarding ice sheet dynamics, a couple of studies suggested the removal of regolith as the mechanism that led to ice sheet growth following the MPT (Clark et al., 2006; Willeit et al., 2019). Both studies (Clark et al., 2006; Willeit et al., 2019) suggested that regolith caused by extensive weathering over 100 Myrs led to more mobile, thinner ice sheets susceptible to orbital forcing. Once the regolith was removed, higher friction induced by Precambrian bedrock led to thicker ice sheets, which drove a change in orbital forcing response from 41 kyr to 100 kyr periodicity (Clark et al., 2006). Regarding global energy budget adjustments, a study by Farmer et al. (2019) suggested a tight linkage between Atlantic Ocean meridional overturning and deep-ocean carbon storage. In the study, they found that carbon inventory increased by 50 gigatons during the MPT, which facilitated deep ocean carbon storage, lowering CO_2 concentrations and enabling the observed expansion of continental ice sheets following the MPT (Farmer et al., 2019).

Pleistocene Glacial Retreat

Deglaciation following the Last Glacial Maximum (LGM) began approximately 19 ka, culminating in significant decreases to large continental ice sheets, such as the Laurentide and Cordilleran Ice Sheets, as well as a global sea level rise of around 120 meters (Shakun and Carlson, 2010; Smith et al., 2011). This period was highlighted by two primary events: the Bølling/Allerød (14.7–12.9 ka) and the Younger Dryas (12.9–11.7 ka) (reference Figure 1c). Ultimately, the PGR filtered into the current Holocene epoch, which is considered an interglacial within the Quaternary Period.

Three primary mechanisms are offered to explain observations during the PGR: CO_2 increase, Boreal summer insolation increase, and Atlantic meridional overturning circulation intensification (Shakun and Carlson, 2010). According to Shakun and Carlson (2010):

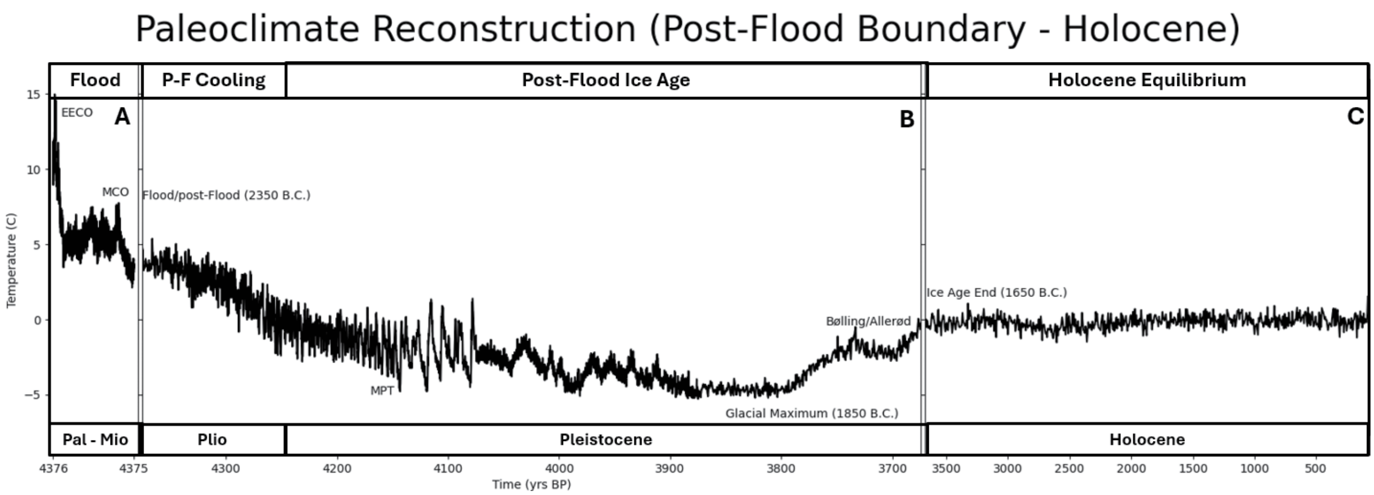

Figure 3. Paleoclimate record compressed into the Biblical timeline from the middle of the flood (~4376 BP) through the Holocene Epoch. Major secular climatic events (labelled in figure) are provided to orient the reader to the data. Notice the timeline is non-linear, meaning Box A represents the end of the Flood year (~7 months), Box B represents the 700-years from the Flood/post-Flood Boundary to the end of the Ice Age, and Box C represents the Holocene Epoch (~3675 years). The 0°C line on the temperature axis is based on the Pre-Industrial Average.

> "The similar timing of the LGM and [deglaciation] between the Northern and Southern Hemispheres suggests that the hemispheres were synchronized at orbital timescales. Atmospheric greenhouse gases are the most likely synchronizer given their global nature."

However, they do note that deglaciation in most records began before CO_2 rose, which signifies CO_2 is a feedback mechanism rather than a cause. Therefore, Shakun and Carlson (2010) suggest that Boreal summer insolation explains the shift toward an interglacial 19–22 ka, while CO_2 increase reinforces the long-term warming pattern. The third mechanism, Atlantic meridional overturning circulation intensification, explains the bipolar seesaw pattern observed in the Northern and Southern Hemispheres. According to Shakun and Carlson (2010), "The Bølling/Allerød and Younger Dryas climate oscillations were an expression of this bipolar seesaw with the Antarctic Cold Reversal representing the opposite sign response of the Southern Hemisphere."

Paleoclimatology—Biblical Framework

The secular perspective of paleoclimatology, with its presupposition of millions of years, treats each sustained climate change as a separate global event, requiring independent causal mechanisms, such as CO_2 fluctuations, Milankovitch cycles, or volcanism. In contrast, the Biblical framework interprets the paleoclimate record as reflecting a single, overarching causal mechanism: the Global Flood. Figure 3 illustrates this reinterpretation by mapping the data from Figure 1 onto a Biblical timeline. The Flood/post-Flood Boundary is placed at 4,375 years before present (BP), corresponding to the Masoretic date of the Flood (circa 2350 BC; Wright, 2012). The Glacial Maximum is positioned at 3,875 years BP, 500 years after the Flood/post-Flood Boundary, and the end of the Ice Age is set at 3,675 years BP, 700 years after the Flood/post-Flood Boundary (Oard, 2019).

Flood/Post-Flood Boundary

Based on deep-sea benthic foraminifera curves and previous creationist research, the Flood/post-Flood Boundary resides near the boundary between the Early Cenozoic warm period and the colder Plio-Pleistocene. This follows closely with the Catastrophic Plate Tectonics (CPT) model developed by Baumgardner (2003), which proposes that the breakup of "the fountains of the great deep" drove rapid subduction of oceanic lithosphere resulting in a new ocean floor by the Flood's end. Lithosphere production, as well as immense volcanism spurred by CPT, warmed the world's oceans causing a significant increase in global temperature, as reflected at the Flood/post-Flood Boundary in Figure 3b (Oard, 1990; Hebert, 2013).

Cenozoic oxygen isotope data deposited prior to the Flood/post-Flood

Boundary corresponds to the Flood Year (Figure 3a). Climate interpretations from this interval are unreliable because the standard equations used to convert oxygen isotope ratios to temperature rely on partition functions that assume a relatively constant temperature. While this assumption becomes reasonable after the Flood—especially as time progresses beyond the Flood/post-Flood Boundary—it is implausible during the Flood itself due to extreme, rapidly changing conditions. What can be inferred, though, is that the global climate was warm during and immediately following the Flood.

The actual date (circa 2350 BC) for the Flood/post-Flood Boundary is based on the Masoretic Text; however, the placement of the boundary in the sediment record is based on temperature maxima found in four locations: the EECO, MECO, MCO, and the Miocene/Pliocene. Because of the progressive nature of the Global Flood, temperature spikes likely indicate catastrophic flood processes; therefore, the final "spike" at the Miocene/Pliocene Boundary indicates a reasonable location for the Flood/post-Flood Boundary (see Figure 3b). This location best aligns with previous research indicating a later end to the Flood—although Oard (2013) and Clarey (2017)'s research favors a slightly later Flood/post-Flood boundary between the Pliocene and Pleistocene.

Although oxygen isotope data supports the Miocene/Pliocene Boundary as the Flood/post-Flood Boundary, its exact placement remains the subject of debate. Positive feedback mechanisms in the climate system—particularly within the carbon cycle—could extend warming beyond the end of the Flood, making a boundary near the EECO plausible. However, CPT-induced subduction zone volcanism complicates this timing, as volcanic aerosols (e.g., SO_2) provide a negative feedback on warming. Consequently, the observed temperature trend depends strongly on climate sensitivity to both CO_2 and volcanic aerosols. Further research is needed to establish baseline sensitivities, which would allow for a more precise placement of the Flood/post-Flood Boundary. Regardless, the paleoclimate record consistently supports a boundary located above the Cretaceous Period.

Post-Flood Cooling

Rapid plate subduction associated with CPT subsided following the Flood; however, vast volcanism continued as the Earth equilibrated, providing a mechanism for rapid cooling of the Earth's climate. According to Abbot and Davies (2012), 1.927 volcanic events are observed in the Greenland Ice Sheet during the Ice Age portion. Data indicate that a single volcanic eruption can produce regional cooling of approximately 0.5°C to 2.5°C. Accordingly, the immense volcanism during the ~500 years between the Flood and the Ice Age maximum likely drove the sustained cooling observed in Figure 3b (Oard, 2019). Additionally, during this period, warm oceans led to increased evaporation and higher snowfall rates on cold mid- and high-latitude land surfaces (Hebert, 2017). Ultimately, it was the coupling of both subduction zone volcanism and increased evaporation that provided the ingredients necessary for the Ice Age, namely cooler summers and increased high latitude precipitation (Oard, 2019).

The rapid post-Flood global cooling observed in this study is consistent with Vardiman (1996), though the rate of cooling is higher due to the compressed timeline of the post-Flood Ice Age. Specifically, the temperature decline from the Flood/post-Flood Boundary to the Ice Age maximum is –0.20°C per decade, approximately 0.06°C per decade faster than Vardiman (1996)'s estimate. By comparison, the magnitude of this natural cooling (0.20°C per decade) is slightly lower than the magnitude of the +0.26°C per decade currently attributed to anthropogenic forcing (Forster et al., 2024). Figure 4 provides a representative depiction of the rapid cooling following the Flood/post-Flood Boundary.

Post-Flood Ice Age

Creationists have conducted considerable research on the post-Flood Ice Age (Hebert, 2013; Clarey, 2019; Oard, 2019; Gollmer, 2023). Although secular scientists propose five major ice ages in Earth history—Mid Precambrian, Late Precambrian, Late Ordovician, Late Paleozoic, and Pleistocene—the sedimentary data from which they infer the first four strongly suggests underwater landslides rather than ice advances (Oard, 2019). This leaves only the Pleistocene Ice Age, an icehouse climate that lasted ~585 years, from the beginning of the Pleistocene Ice Age to the Holocene (reference Figure 3b).

Often referred to as the HEAT model, the Biblical framework of the Ice Age better explains Pleistocene climate (Hebert, 2013). Rather than proposing multiple mechanisms, such as "tipping points" for the transition from greenhouse to icehouse climate (i.e., the Eocene/Oligocene Boundary) or Milankovitch cycles as the pacemaker of glacial-interglacial periods, the Global Flood provides a powerful, singular mechanism to explain the whole of the paleoclimate record, from observed Eocene through Pleistocene cooling to Glacial Maximum and finally to the Ice Age's conclusion (Hebert, 2013; Oard, 2019).

Secular scientists interpret the Pleistocene Ice Age as containing multiple glacial-interglacial cycles (Figures 2a–2b), with the current Holocene Epoch considered an interglacial embedded within this Ice Age (Berger and Loutre, 2002). In contrast, creationists

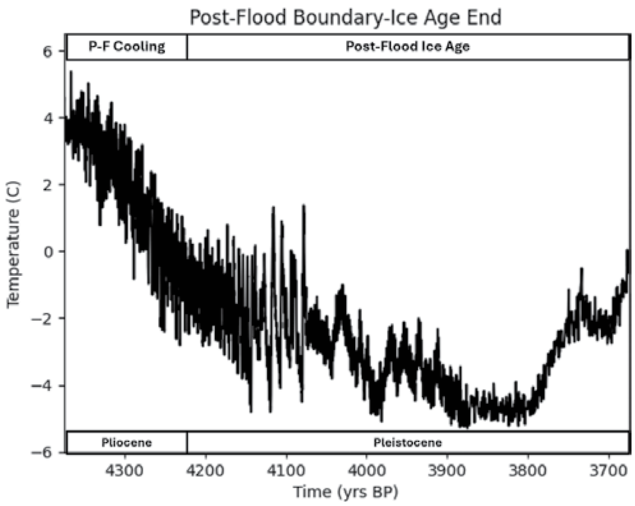

Figure 4. Temperature reconstruction from the Flood/post-Flood Boundary to the end of the Pleistocene Ice Age. This graphic depicts the rapid -0.20°C per decade cooling, as well as the +0.26°C per decade warming following the end of the Global Flood.

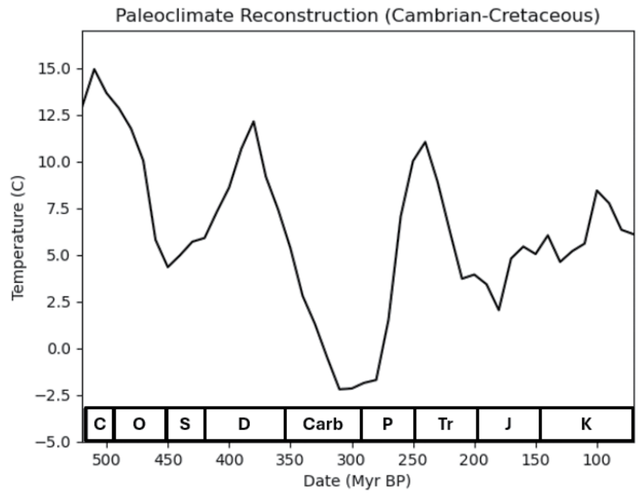

Figure 5. Paleoclimate record during the Flood year from the Cambrian to the Cretaceous. The 0°C line on the temperature axis is based on the Pre-Industrial Average.

argue that these glacial-interglacial cycles are a misinterpretation of ice core records, particularly in the lower portions where annual layers are not preserved (Hebert, 2018). Figure 3b shows the period from the Flood/post-Flood Boundary to the end of the Ice Age. While the glacial-interglacial cycles remain visible even after timeline compression, a reinterpretation of oxygen isotope ratios would likely smooth the curve, as chemical variations at depth reflect shorter-term fluctuations—seasonal or even single-storm events—rather than decade- or century-scale climate changes. Future research will focus on reinterpreting ice core-derived temperatures within the Biblical Ice Age framework.

Ice Age End

According to secular scientists, Earth currently resides in the Holocene interglacial period. The Biblical framework, on the other hand, suggests this "interglacial" is a recovery of the climate system to a post-Flood equilibrium state (see Figure 3c). Following the cessation of CPT, residual catastrophism from the Flood declined to the currently observed rates, the ocean thermohaline circulation balanced, and volcanic aerosols were removed from the stratosphere, all allowing for the climate system to reach the equilibrium state observed for approximately 3,675 years (reference Figure 3c).

Like the rapid cooling trend (reference "Post-Flood Cooling" section), evidence for the strength of natural forcing is also observed in rapid warming from Glacial Maximum to the beginning of the Holocene. During this period, the Earth's climate witnessed a +0.27°C per decade increase in temperature. This rate is 0.01°C greater than current estimates of anthropogenic forcing, which indicates that natural forcing is much stronger than currently assessed.

Discussion

Earlier Climate Records

This paper focuses on the paleoclimate record from the Flood/post-Flood Boundary to the end of the Ice Age (i.e., Cenozoic Era); however, climate reconstructions do exist for the Flood Year. One study often referenced in paleoclimate records is Royer et al. (2004), which provides oxygen isotope ratios extending back to the Devonian Period. Figure 5 displays the Royer et al. (2004) temperature reconstruction derived from oxygen isotope ratios, which stretches from the Devonian Period through the Cretaceous. Although a warming trend emerges following the Triassic/Jurassic Boundary, inferring climatic trends from sediments during the Global Flood is impractical; therefore, these datasets were purposefully omitted.

Volcanism

Secular scientists associate volcanism with many global warming periods in the paleoclimate record (Gutjahr et al., 2018; Kasbohm and Schoene, 2018; van der Boon et al., 2021). They claim CO_2 increases stem from many major volcanic eruptions occurring over periods of thousands to millions of years. Creationists observe the same volcanism in the geologic record; however, the short Biblical timeline allows eruptions during and immediately following the Flood to function as a cooling mechanism for post-Flood climates. Secular scientists cannot draw these same conclusions because of their commitment to millions of years; therefore, they struggle to explain the origin of the Ice Age.

Climate Change

Periods such as the EECO are frequently used by secular scientists to compare Representative Concentration Pathways (RCPs) to past climates. One study projected that under RCP 8.5, "[future climates would] most closely resemble [the] Eocene" by 2150, with CO_2 concentrations reaching 1,200–2,500 ppmv (Burke et al., 2018; Lunt et al., 2021). However, the likelihood of achieving Eocene-level warming is extremely low, as events like the PETM and EECO were consequences of a unique, never-to-be-repeated Global Flood. This is not to imply that climate change is fabricated—particularly not the IPCC's moderate RCP scenarios—but rather to counter claims of catastrophic climate change, which God has promised will never occur again (Genesis 8:22). Less extreme radiative forcing pathways, such as RCP2.6, are projected to produce climates similar to the Pliocene (~5–3 Ma) by the end of the century (Steinthorsdottir et al., 2020).

Secular scientists claim anthropogenic forcing is rapidly altering the equilibrium state observed throughout the Holocene epoch. Alarming claims of catastrophic climate change fill media headlines; however, creationists believe these stem from a gross misinterpretation of the paleoclimate record. Because secular scientists assume CO_2 concentrations drive major climate changes, they predict Earth could be headed toward unlivable conditions, if humans do not curb emissions. Hansen et al. (2013) perfectly sum up the secular fear of climate change in their closing discussion on global habitability. According to Hansen et al. (2013):

> "The Earth was 10–12°C warmer than today in the Early Eocene and at the peak of the PETM. How did mammals survive that warmth? Some mammals have higher internal temperatures than humans, and there is evidence of evolution of surface-area-to-mass ratio to aid heat dissipation…However, human-made warming will occur in a few centuries, as opposed to several millennia in the PETM, thus providing little opportunity for evolutionary dwarfism to alleviate the impacts of global warming. [The authors] conclude that the large climate change from burning all fossil fuels would threaten the biological health and survival of humanity, making policies that rely substantially on adaptation inadequate."

Biblical creationists do not share this same fear because we know the paleoclimate record tells a vastly different story. If secular scientists would simply start from the actual historical record of origins, rather than the theories of evolution and uniformitarianism, they would see that the paleoclimate record points to the catastrophic Global Flood!

Conclusion

In this study, it was shown that secular paleoclimate reconstructions provide compelling evidence for the Biblical framework. Of course, interpretations of deep-sea sediments are subject to human error, especially when created with uniformitarianism in mind, but thankfully, Christians also have the infallible Word of God to support our interpretation of the paleoclimate record. Furthermore, Christians have the Word of God to support claims against catastrophic climate change. After Noah and his family exited the Ark and sacrificed offerings on the altar, God promised that he would "not again curse the ground…for man's sake" (Genesis 8:21). Furthermore, God told Noah that "while the earth remains, seedtime and harvest, and cold and heat, and summer and winter, and day and night shall not cease" (Genesis 8:22). When the paleoclimate record is reexamined through the lens of Scripture, the Flood and its aftermath provide a causally sufficient, theologically consistent, and scientifically coherent explanation of Earth's climate history—one that secular models, with their reliance on deep time and unstable cycles, fail to achieve.

References

Anagnostou, E., E.H. John, K.M. Edgar, G.L. Foster, A. Ridgwell, G.N. Inglis, R.D. Pancost, D.J. Lunt, and P.N. Pearson (2016). Changing atmospheric CO_2 concentration was the primary driver of Early Cenozoic climate. *Nature* 533:380–384.

Bartoli, G., B. Honisch, and R.E. Zeebe. 2011. Atmospheric CO_2 decline during the Pliocene intensification of Northern Hemisphere glaciations. *Paleoceanography* 26(4).

Baumgardner, J.R. 2003. Catastrophic plate tectonics: The physics behind the Genesis Flood. *International Conference on Creationism*, Volume 5. Creation Science Fellowship, Pittsburgh, PA.

Berger, A., and M.F. Loutre. 2002. An exceptionally long interglacial ahead? *Science* 297(5585):1287–1288.

Bohaty, S.M., J.C. Zachos, F. Florindo, and M.L. Delaney. 2009. Coupled greenhouse warming and deep-sea acidification in the Middle Eocene. *Paleoceanography* 24(2).

Bohaty, S.M., and J.C. Zachos. 2003. Significant Southern Ocean warming event in the Late Middle Eocene. *Geology* 31(11):1017–1020.

Burke, K.D., J.W. Williams, M.A. Chandler, A.M. Haywood, D.J. Lunt, B.L.

Otto-Bliesner 2018. Pliocene and Eocene provide best analogs for near-future climates. *Proceedings of the National Academy of Sciences* 115(52):13288–13293.

Chalk, T.B., M.P. Hain, G.L. Foster, E.J. Rohling, P.F. Sexton, M.P.S. Badger, S.G. Cherry, A.P. Hasenfratz, G.H. Haug, S.L. Jaccard, A. Martinez-Garcia, H. Palike, R.D. Pancost, and P.A. Wilson. 2017. Causes of Ice Age intensification across the Mid-Pleistocene Transition. *Proceedings of the National Academy of Sciences* 114(50):13114–13119.

Clarey, T. 2017. Local catastrophes or receding Floodwater? Global geologic data that refute a K-Pg (K-T) Flood/post-Flood Boundary. *CRSQ* 54(1):100–120.

Clarey, T. 2019. Subduction was essential for the Ice Age. *Acts and Facts* 48(3).

Clark, P.U., D. Archer, D. Pollard, J.D. Blum, J.A. Rial, V. Brovkin, A.C. Mix, N.G. Pisias, and M. Roy. 2006. The Middle Pleistocene Transition: Characteristics, mechanisms, and implications for long-term changes in atmospheric pCO2. *Quaternary Science Review* 25(23–24):3150–3184.

Coxall, H.K., and P.N. Pearson. 2007. The Eocene-Oligocene Transition. *Deep-Time Perspectives on Climate Change: Marrying the Signal from Computer Models and Biological Proxies*. Geological Society of London, London, UK.

DeConto, R.M., and D. Pollard. 2003. Rapid Cenozoic glaciation of Antarctica induced by declining atmospheric CO2. *Nature* 421:245–249.

De Schepper, S., P.L. Gibbard, U. Salzmann, and J. Ehlers. 2014. A Global Synthesis of the Marine and Terrestrial Evidence for Glaciation During the Pliocene Epoch. *Earth-Science Review* 135:83–102.

Farmer, J.R., B. Honisch, L.L. Haynes, D. Kroon, S. Jung, H.L. Ford, M.E. Raymo, M. Jaume-Segui, D.B. Bell, S.L. Goldstein, L.D. Pena, M. Yehudai, and J. Kim. 2019. Deep Atlantic Ocean carbon storage and the rise of 100,000-year glacial cycles. *Nature Geoscience* 12:355–360.

Forster, P.M., C. Smith, T. Walsh, W.F. Lamb, R. Lamboll, B. Hall, M. Hauser, A. Ribes, D. Rosen, N.P. Gillett, M.D. Palmer, J. Rogelj, K. von Schuckmann, B. Trewin, M. Allen, R. Andrew, R.A. Betts, A. Borger, and T. Boyer. 2024. Indicators of global climate change 2023: Annual update of key indicators of the state of the climate system and human influence. *Earth System Science Data* 16(6):2625–2658.

Giorgioni, M., L. Jovane, E.S. Rego, D. Rodelli, F. Frontalini, R. Coccioni, R. Catanzariti, and E. Ozcan. 2019. Carbon cycle instability and orbital forcing during the Middle Eocene Climatic Optimum. *Scientific Reports* Volume 9. Creation Science Fellowship, Pittsburgh, PA.

Gollmer, Steven M. 2023. A rapid Ice Age and transition to ice sheet growth. *International Conference on Creationism* 9:267–279.

Goto, K.T., M.L.G. Tejada, E. Tajika, and K. Suzuki. 2023. Enhanced magmatism played a dominant role in triggering the Miocene Climatic Optimum. *Communications Earth and Environment,* Volume 4.

Gutjahr, M., A. Ridgwell, P.F. Sexton, E. Anagnostou, P.N. Pearson, H. Palike, R.D. Norris, E. Thomas, and G.L. Foster. 2018. Very large release of mostly volcanic carbon during the Paleocene-Eocene Thermal Maximum. *Nature* 548(7669):573–577.

Hamon, N.P. Sepulchre, V. Lefebvre, and G. Ramstein. 2013. The role of Eastern Tethys Seaway closure in the Middle Miocene Climatic Transition (ca. 14 Ma). *Climates of the Past* 9(6):2687–2702.

Hansen, J., M. Sato, G. Russell, and Kharecha, P. 2013. Climate sensitivity, sea level, and atmospheric carbon dioxide. *Philosophical Transactions of the Royal Society,* Volume 371.

Haynes, L.L., and B. Honisch, 2020. The seawater carbon inventory at the Paleocene-Eocene Thermal Maximum. *Proceedings of the National Academy of Sciences* 117(39):24088–24095.

Haywood, A.M., P.J. Valdes, T. Aze, N. Barlow, A. Burke, A.M. Dolan, A.S. von der Heydt, D.J. Hill, S.S.R. Jamieson, B.L. Otto-Bilesner, U. Salzmann, E. Saupe, J. Voss. 2019. What Can Paleoclimate Modelling Do for You? *Earth Systems and Environment* 3:1–18.

Hebert, J. 2014. Circular reasoning in the dating of deep seafloor sediments and ice cores: The orbital tuning method. *Answers Research Journal* 7:297–309.

Hebert, J. 2018. Tephra and inflated ice core ages. *Journal of Creations* 32(3):4–6.

Hebert, J. 2013. Was there an Ice Age? *Acts and Facts* 42(12).

Hren, M.T., N.D. Sheldon, S.T. Grimes, M.E. Collinson, J.J. Hooker, M. Bugler, and K.C. Lohmann. 2013. Terrestrial cooling in Northern Europe during the Eocene-Oligocene Transition. *Proceedings of the National Academy of Sciences* 110(19):7562–7567.

Inglis, G.N., F. Bragg, N.J. Burls, M.J. Cramwinckel, D. Evans, G.L. Foster, M. Huber, D.J. Lunt, N. Siler, S. Steinig, and J.E. Tierney. 2020. Global mean surface temperature and climate sensitivity of the Early Eocene Climatic Optimum (EECO), Paleocene-Eocene Thermal Maximum (PETM), and Latest Paleocene. *Chemical Geology* 211(1–2):47–69.

Jimenez-Moreno, G.J.N. Perez-Asensio, J.C. Larrasoana, F.J. Sierro, D. Garcia-Castellanos, A. Salazar, J.M. Salvany, S. Ledesma, M.P. Mata, and C. Mediavilla. 2019. Early Pliocene Climatic Optimum, cooling and early glaciation deduced by terrestrial and marine environmental changes in SW Spain. *Global and Planetary Change* 180:89–99.

Jones, S.M., M. Hoggett, S.E. Greene, and T.D. Jones. 2019. Large igneous province thermogenic greenhouse gas flux could have initiated Paleocene-Eocene Thermal Maximum climate change. *Nature Communications* Volume 10.

Jouzel, J., V. Masson-Delmotte, O. Cattani, G. Dreyfus, S. Falourd, G. Hoffman, B. Minster, J. Nouet, J.M. Barnola, J. Chappellaz, H. Fischer, J.C. Gallet, S. Johnsen, M. Leuenberger, L. Loulergue, D. Luethi, H. Oerter, F. Parrenin, G. Raisbeck, D. Raynaud, A. Schilt, J. Schwander, E. Selmo, R. Souchez, R. Spahni, B.

Stauffer, J.P. Steffenson, B. Stenni, T.F. Stocker, J.L. Tison, M. Werner, and E.W. Wolff. 2007. Orbital and millennial Antarctic climate variability over the past 800,000 years. *Science* 317:793–796.

Kasbohm, J., and B. Schoene. 2018. Rapid eruption of the Columbia River flood basalt and correlation with the Mid-Miocene Climate Optimum. *Science Advances* 4(9).

Katz, M.E., K.G. Miller, J.D. Wright, B.S. Wade, J.V. Browning, B.S. Cramer, and Y. Rosenthal 2008. *Nature Geoscience* 1:329–334.

Lauretano, V., K. Littler, M. Polling, J.C. Zachos, and L.J.Lourens. 2015. Frequency, magnitude, and character of hyperthermal events at the onset of the Early Eocene Climatic Optimum. *Climates of the Past* 11(10):1313–1324.

Lawrence, K.T., S. Sosdian, H.E. White, and Y. Rosenthal. 2010. North Atlantic climate evolution through the Plio-Pleistocene climate transitions. *Earth and Planetary Science Letters* 300(3–4):329–342.

Lisiecki, L.E., and Raymo, M.E. 2005. A Pliocene-Pleistocene stack of 57 globally distributed benthic δ18O records. *Paleoceanography* 20(1).

Liu, Z., M. Pagani, D. Zinniker, R. Deconto, M. Huber, H. Brinkhuis, S.R. Shah, R.M. Leckie, and A. Pearson. 2009. Global cooling during the Eocene-Oligocene Climate Transition. *Science* 323(5918):1187–1190.

Lunt, D.J., F. Bragg, W. Chan, D.K. Hutchinson, J. Ladant, P. Morozova, I. Niezgodzki, S. Steinig, Z. Zhang, J. Zhu, A. Abe-Ouchi, E. Anagnostou, A.M. de Boer, H.K. Coxall, Y. Donnadieu, G. Foster, G.N. Inglis, G. Knorr, P.M. Langebroek, C.H. Lear, G. Lohmann, C.J. Poulsen, P. Sepulchre, J.E. Tierney, P.J. Valdes, E.M. Volodin, T.D. Jones, C.J. Hollis, M. Huber, and B.L. Otto-Bliesner. 2021. DeepMIP: Model intercomparison of Early Eocene Climatic Optimum (EECO) large-scale climate features and comparison with proxy data. *Climates of the Past* 17(1):203–227.

McInerney, F.A., and S.L. Wing. The Paleocene-Eocene Thermal Maximum: A perturbation of carbon cycle, climate, and biosphere with implications for the future. *Annual Review of Earth and Planetary Sciences* 39:489–516.

McKay, D.I.A., T. Tyrrell, P.A. Wilson, and G.L. Foster. 2014. Estimating the impact of the cryptic degassing of large igneous provinces: A Mid-Miocene case study. *Earth and Planetary Science Letters* 403:254–262.

Oard, M.J. 1990. *An Ice Age Caused by the Genesis Flood*. Institute for Creation Research, El Cajon, CA.

Oard, M.J. 2005. *The Frozen Record: Examining the Ice Core History of the Greenland and Antarctic Ice Sheets.* Institute for Creation Research, Dallas, TX.

Oard, M.J. 2013. Geology indicates the terrestrial Flood/post-Flood boundary is mostly in the Late Cenozoic. *Journal of Creation* 27(1):119–127.

Oard, M.J. 1984. Ice Ages: The mystery solved? Part II: The manipulation of deep-sea cores. *Creation Research Society Quarterly* 21(3):125–137.

Oard, M.J. 2020. Ice core oscillations and abrupt climate changes: Part 1—Greenland ice cores. *Journal of Creation* 34(3):99–108.

Oard, M.J. 2019. The unique post-Flood Ice Age. *Creation* 41(4):44–47.

Pagani, M., J.C. Zachos, K.H. Freeman, B. Tipple, and S. Bohaty. 2005. Marked decline in atmospheric carbon dioxide concentrations during the Paleogene. *Science* 309(5734):600–603.

Pearson, P.N. 2010. Increased atmospheric CO_2 during the Middle Eocene. *Science* 330(6005):763–764.

Piedrahita, V.A., S. Galeotti, X. Zhao, A.P. Roberts, E.J. Rohling, D. Heslop, F. Florindo, K.M. Grant, L. Rodriguez-Sanz, D. Reghellin, and R.E. Zeebe. 2022. Orbital phasing of the Paleocene-Eocene Thermal Maximum. *Earth and Planetary Science Letters* 598(15).

Raitzsch, M., J. Bijma, T. Bickert, M. Schulz, A. Holbourn, and M. Kucera. 2021. Atmospheric carbon dioxide variations across the Middle Miocene Climate Transition. *Climates of the Past* 17(2):703–719.

Raymo, M.E. 1994. The Himalayas, organic carbon burial, and climate in the Miocene. *Paleoceanography* 9(3):399–404.

Rosman, K.J.R., and P.D.P. Taylor. 1998. Isotopic compositions of the elements (technical report): Commission on atomic eeights and isotopic abundances. *Pure and Applied Chemistry* 70(1):217–235.

Schmidt, Gavin (2014). Can we make better graphs of global temperature history? *Real Climate*. https://www.realclimate.org/index.php/archives/2014/03/can-we-make-better-graphs-of-global-temperature-history/.

Shakun, J.D., and A.E. Carlson. 2010. A global perspective on Last Glacial Maximum to Holocene climate change. *Quaternary Science Reviews* 29(15–16):1801–1816.

Slujis, A., H. Brinkhuis, S. Schouten, S.M. Bohaty, C.M. John, J.C. Zachos, G. Reichart, J.S. Sinninghe Damste, E.M. Crouch, and G.R. Dickens (2007). Environmental precursors to rapid light carbon injection at the Palaeocene/Eocene Boundary. *Nature* 450:1218–1221.

Slujis, A., P.K. Bijl, S. Schouten, U. Rohl, G.J. Reichart, and H. Brinkhuis. 2011. Southern Ocean warming, sea level, and hydrological change during the Paleocene-Eocene Thermal Maximum. *Climate of the Past* 7(1):47–61.

Smith, D.E., S. Harrison, C.R. Firth, and J.T. Jordan. 2011. The Early Holocene sea level rise. *Quaternary Science Reviews* 30(15–16):1846–1860.

Sosdian, S.M., T.L. Babila, R. Greenop, G.L. Foster, and C.H. Lear. 2020. Ocean carbon storage across the Middle Miocene: A new interpretation for the Monterey Event. *Nature Communications,* Volume 11.

Steinthorsdottir, M., H.K. Coxall, A.M. de Boer, M. Huber, N. Barbolini, C.D. Bradshaw, N.J. Burls, S.J. Feakins, E. Gasson, J. Henderiks, A.E. Holbourn, S. Kiel, M.J. Kohn, G. Knorr, W.M.

Kurschner, C.H. Lear, D. Liebrand, D.J. Lunt, T. Mors, P.N. Pearson, M.J. Pound, H. Stoll, and C.A.E. Stromberg. 2020. The Miocene: The future of the past. *Paleoceanography and Paleoclimatology* 36(4).

Tierney, J.E., J. Zhu, M.Li, A. Ridgwell, G.J. Hakim, C.J. Poulsen, R.D.M. Whiteford, J.W.B. Rae, L.R. Kump. 2022. Spatial patterns of climate change across the Paleocene-Eocene Thermal Maximum. *Proceedings of the National Academy of Sciences* 119(42).

Van der Boon, A., K.F. Kuiper, R. van der Ploeg, M.J. Cramwinckel, M. Honarmand, A. Slujis, and W. Krijgsman. 2021. Exploring a link between the Middle Eocene Climatic Optimum and Neotethys continental arc flare-up. *Climate of the Past* 17(1):229–239.

Vardiman, L. 1997. Rapid changes in oxygen isotope content of ice cores caused by fractionation and trajectory dispersion near the edge of an ice shelf. *Journal of Creation* 11(1):52–60.

Vardiman, L. 1996. The sands of time: A Biblical model of deep sea-floor sedimentation. *Creation Research Society Quarterly* 33(3):191–198.

Vincent, E., J.S. Killingsley, and W.H. Berger. 1985. Miocene oxygen and carbon isotope stratigraphy of the tropical Indian Ocean. *The Miocene Ocean: Paleoceanography and Biogeography*. https://pubs.geoscienceworld.org/gsa/books/edited-volume/172/chapter-abstract/3792450/Miocene-oxygen-and-carbon-isotope-stratigraphy-of?redirectedFrom=fulltext.

Westerhold, T., and U. Rohl. 2013. Orbital pacing of Eocene climate during the Middle Eocene Climate Optimum and the Chron C19r Event: Missing link found in the tropical Western Atlantic. *Geochemistry, Geophysics, Geosystems* 14(11):4811–4825.

Willeit, M., A. Ganopolski, R. Calov, and V. Brovkin. 2019. Mid-Pleistocene Transition in glacial cycles explained by declining CO_2 and regolith removal. *Science Advances* 5(4).

Woodruff, F., and S.M. Savin. 1989. Miocene deepwater oceanography. *Paleoceanography* 4:87–140.

Wright, D. 2012. Timeline for the Flood. *Answers in Genesis*. https://answersingenesis.org/bible-timeline/timeline-for-the-flood/

Wright, J.D., K.G. Miller, and R.G. Fairbanks. 1992. Early and Middle Miocene stable isotopes: Implications for deepwater ocean circulation and climate. *Paleoceanography* 7:357–389.

Zachos, J.C., Dickens, G.R., and Zeebe, R.E. 2008. An Early Cenozoic perspective on greenhouse warming and carbon-cycle dynamics. *Nature* 451:279–283.

Zhang, S., W. Ji, H. Chen, L.A. Kirstein, and F. Wu. 2023. Linking rapid eruption of the Linzizong volcanic rocks and Early Eocene Climatic Optimum (EECO): Constraints from the Pana Formation in the Linzhou and Pangduo Basins, Southern Tibet. *Lithos* Volumes 446–447:107159.